iScience

CellPress
OPEN ACCESS

Article

Hippocampal 7α-Hydroxylated Neurosteroids Are Raised by Training and Bolster Remote Spatial Memory with Increase of the Spine Densities

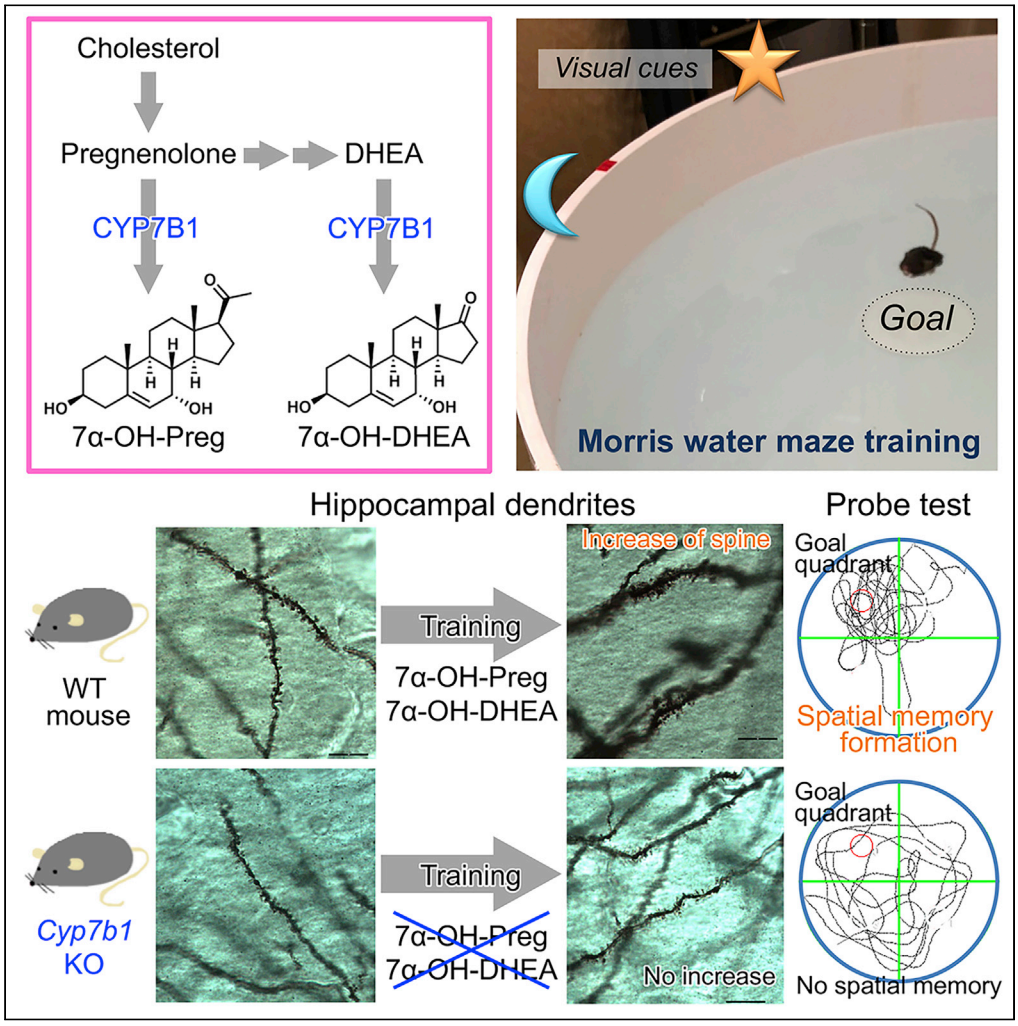

Kanako Maehata, Kimiko Shimizu, Tomoko Ikeno, ..., Yue Pan, Toshifumi Takao, Yoshitaka Fukada

shimizuk@bs.s.u-tokyo.ac.jp (K.S.)
sfukada@mail.ecc.u-tokyo.ac.jp (Y.F.)

HIGHLIGHTS

LC-MS/MS analysis identified 7α-hydroxylated neurosteroids in the mouse hippocampus

The hippocampal neurosteroids were induced by spatial water maze training

KO of 7α-hydroxylating enzyme impaired remote memory and hippocampal spine density

Infusion of the 7α-hydroxylated steroids to the KO rescued impaired remote memory

Maehata et al., iScience 23, 101559
October 23, 2020
https://doi.org/10.1016/j.isci.2020.101559

iScience

CellPress
OPEN ACCESS

Article

Hippocampal 7α-Hydroxylated Neurosteroids Are Raised by Training and Bolster Remote Spatial Memory with Increase of the Spine Densities

Kanako Maehata,[1,3] Kimiko Shimizu,[1,3,4,*] Tomoko Ikeno,[1] Qiuyi Wang,[2] Ayaka Sakurai,[1] Zefeng Wei,[1] Yue Pan,[2] Toshifumi Takao,[2] and Yoshitaka Fukada[1,*]

SUMMARY

Neuroactive steroids, termed neurosteroids, are synthesized locally in the brain and influence biological functions including cognition and behavior. These neurosteroids are synthesized from cholesterol by a series of cytochrome P450 enzymes, among which a member of P450 hydroxylase, cytochrome P450-7b1 (CYP7B1), catalyzes the formation of 7α-hydroxylated neurosteroids, 7α-hydroxypregnenolone (7α-OH-Preg) and 7α-hydroxydehydroepiandrosterone (7α-OH-DHEA). Here we demonstrated the occurrence of these neurosteroids in the mouse hippocampus after spatial-learning tasks. *Cyp7b1* deficiency impaired remote spatial memory with recent memory mostly unaffected. The hippocampal dendritic spine densities were reduced in *Cyp7b1*-deficient mice, and they were no more increased by the training. Furthermore, chronic intracerebroventricular administration of a mixture of 7α-OH-Preg and 7α-OH-DHEA rescued the deteriorated remote memory performance in *Cyp7b1*-deficient mice. It is concluded that the 7α-hydroxylated neurosteroids are required for long-term maintenance of spatial memory, and we suggest that these neurosteroids may induce synaptic remodeling to maintain the hippocampal function.

INTRODUCTION

The brain now comes into focus as a steroidogenic organ producing neurosteroids (Corpéchot et al., 1981; Akwa et al., 1992). Neurosteroids are implicated in a variety of brain functions such as cognition and behavior (Baulieu, 2000; El Kihel, 2012; Tsutsui et al., 2013; Wingfield et al., 2018), although their biological roles in mammals are not fully understood. Neurosteroids are synthesized from cholesterol, which is transferred to the mitochondria by steroidogenic acute regulatory protein (StAR) as the first step of steroidogenesis (Figure 1A). Then cholesterol is converted into pregnenolone, a common precursor of neurosteroids, by cholesterol monooxygenase (CYP11A1; also termed P450scc, cholesterol side chain-cleaving enzyme). Pregnenolone is subsequently converted into various bioactive steroids by hydroxylation and/or oxidation (Akwa et al., 1992; Wingfield et al., 2018; Morfin and Courchay, 1994; Payne and Hales, 2004). Cytochrome P450-7b1 (CYP7B1) catalyzes the hydroxylation of pregnenolone at the 7α-position, and therefore CYP7B1 is essential for the biosynthesis of 7α-hydroxypregnenolone (7α-OH-Preg) (Rose et al., 1997). Another neurosteroid synthesized by CYP7B1 is 7α-hydroxydehydroepiandrosterone (7α-OH-DHEA) (Rose et al., 1997). The biosynthetic pathway of 7α-OH-DHEA involves CYP17A1-catalyzed two-step conversion of pregnenolone into dehydroepiandrosterone (DHEA), which is then 7α-hydroxylated by CYP7B1 to form 7α-OH-DHEA (Figure 1A). *Cyp7b1* mRNA is detected widely in mouse tissues by *in situ* hybridization, with high levels in the liver and kidney and particularly high levels in the dentate gyrus (DG) of the hippocampus (Rose et al., 2001).

Intracerebroventricular infusion of 7α-OH-Preg into aged rats ameliorates the spatial memory impairment (Yau et al., 2006), but *in vivo* occurrence of 7α-OH-Preg in the mammalian brain has been an issue of debate. On the other hand, 7α-OH-DHEA was identified in the ventricular cerebrospinal fluid of humans (Stárka et al., 2009). Although 7α-OH-DHEA has not been detected in the rodent brain, 7α-hydroxylating activity on DHEA is distributed among a variety of tissues, including the rodent brain (Morfin and Courchay, 1994; Rose et al., 2001). In culture, 7α-OH-DHEA has a neuroprotective effect on ischemia-induced rat

[1]Department of Biological Sciences, School of Science, The University of Tokyo, Hongo 7-3-1, Bunkyo-ku, Tokyo 113-0033, Japan

[2]Institute for Protein Research, Osaka University, Yamadaoka 3-2, Suita-shi, Osaka 565-0871, Japan

[3]These authors contributed equally

[4]Lead Contact

*Correspondence: shimizuk@bs.s.u-tokyo.ac.jp (K.S.), sfukada@mail.ecc.u-tokyo.ac.jp (Y.F.)

https://doi.org/10.1016/j.isci.2020.101559

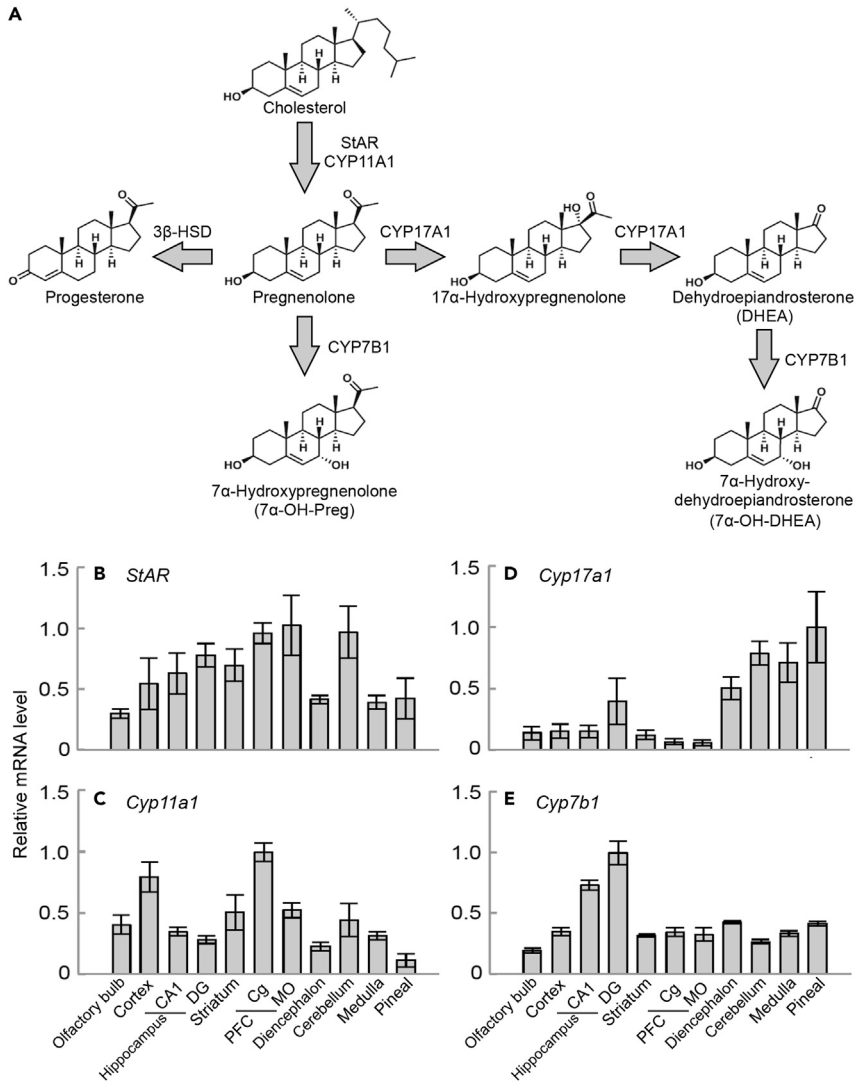

Figure 1. Biosynthesis of Neurosteroids and Expression Profiles of Genes Responsible for Formation of 7α-OH-Preg and 7α-OH-DHEA in Mouse Brain Regions

(A) Biosynthetic pathways of 7α-hydroxylated neurosteroids. StAR transfers cholesterol to the mitochondria, where CYP11A1 catalyzes the conversion of cholesterol into pregnenolone. Pregnenolone is subsequently converted into various neurosteroids by hydroxylation and/or oxidation. Among the pathways, CYP7B1 catalyzes the 7α-hydroxylation of pregnenolone for the formation of 7α-OH-Preg. Alternatively, CYP17A1 catalyzes a two-step 17-oxydation pathway of pregnenolone for the formation of dehydroepiandrosterone (DHEA), which is then 7α-hydroxylated by CYP7B1 to form 7α-OH-DHEA.

(B–E) The expression levels of mRNAs for (B) *StAR*, (C) *Cyp11a1*, (D) *Cyp17a1*, and (E) *Cyp7b1* were quantitated by RT-qPCR analysis of RNA samples prepared from various brain regions. CA1, hippocampal CA1 region; DG, dentate gyrus; Cg, cingulate cortex; MO, medial orbital cortex; PFC, prefrontal cortex. Data are normalized by mRNA levels of *Rps29*. The expression levels were presented as values relative to the maximal level in each panel. Values are shown as the mean ± SEM (n = 3–4).

hippocampal neurons (Pringle et al., 2003). It also should be noted that *Cyp7b1* mRNA is significantly reduced in the dentate neurons of subjects with Alzheimer disease (Yau et al., 2003). In this way, CYP7B1 is considered relevant to higher brain functions, particularly to hippocampus-dependent memory performance.

In this study, we discovered that *Cyp7b1* deficiency in mice impaired long-term maintenance of hippocampus-dependent spatial memory. The impaired remote memory performance was rescued by

intracerebroventricular infusion of both 7α-OH-Preg and 7α-OH-DHEA. Importantly, 7α-OH-Preg and 7α-OH-DHEA were detected in the mouse hippocampus only after the spatial-learning tasks. These results demonstrate that these 7α-hydroxylated neurosteroids are the key mediators of remote memory formation and suggest learning task-induced biosynthesis of these neurosteroids in the mouse hippocampus.

RESULTS

Expression Profiles of Genes Responsible for Neurosteroidogenesis

We investigated the expression levels of mRNAs encoding four proteins responsible for the conversion of cholesterol into 7α-OH-Preg and 7α-OH-DHEA in the mouse brain (Figure 1A). We found that mRNAs for *StAR* (Figure 1B), *Cyp11a1* (Figure 1C), *Cyp17a1* (Figure 1D), and *Cyp7b1* (Figure 1E) were expressed in the various brain regions. mRNA expression levels of *Cyp7b1* were higher in both CA1 and DG of the hippocampus than in the other brain regions, as reported previously (Rose et al., 2001). In the present study, we used *Cyp7b1* knockout (KO) mice (Li-Hawkins et al., 2000), in which biosyntheses of 7α-hydroxylated steroids, 7α-OH-Preg and 7α-OH-DHEA, are blocked. These KO mice were apparently indistinguishable from wild-type (WT) mice.

Spatial Memory Performance of *Cyp7b1* KO Mice

As the expression levels of *Cyp7b1* were relatively high in the CA1 and DG (Figure 1E), we investigated hippocampus-dependent spatial memory performance of *Cyp7b1* KO mice by using the Morris water maze task. The male mice (11–18 weeks) were trained for 5 consecutive days with 4 trials per day. In the training trials, the escape latency (time duration) to reach a hidden platform (Figure 2A) and the swimming distance (Figure 2B) were both decreased on a daily basis. We found no significant difference in the learning curves between *Cyp7b1* KO and the littermate WT mice (Figures 2A and 2B). On the next day after 5-day training trials, the mice were assessed for recent spatial memory by subjecting to a probe test of 60 s (probe test I), in which the hidden platform was removed. Then we measured the time spent in goal (G) quadrant exploring the platform, opposite (O) quadrant, or side (S) quadrant (average time in right- and left-side quadrants). In both genotypes, the stay time in quadrant G was significantly higher than the chance level (25%) (Figure 2C). The stay times in quadrant G were comparable between the two genotypes (Figure 2D), indicating that recent spatial memory was maintained normally in *Cyp7b1* KO mice.

Two weeks after the probe test I, all the mice were subjected to the probe test again (probe test II) for assessing remote spatial memory. We found that WT mice explored quadrant G much longer than the chance level (Figure 2E). In *Cyp7b1* KO mice, on the other hand, the stay time ratio in quadrant G decreased to a level not significantly different from the chance level (Figure 2E). A comparison between the two genotypes demonstrated that remote spatial memory was impaired by *Cyp7b1* deficiency (Figure 2F). In these experiments, the swimming distance and speed in both the probe tests were comparable between the two genotypes, indicating normal physical ability of *Cyp7b1* KO mice (Figures S1A–SD). Consistently, no obvious difference was detected in daily locomotor activities between the genotypes (Figure S2). Also, anxiety-like behaviors of the mutant mice were indistinguishable from WT, as judged from results of the elevated plus maze test (Figures S3A and S3B) and the open field test (Figures S3C and S3D).

Dendritic Spine Analysis in the *Cyp7b1* KO Hippocampus

It is reported that memory formation including remote spatial memory is associated with neuronal structural changes in the hippocampal CA1 and DG (Leuner et al., 2003; Restivo et al., 2009; Mahmmoud et al., 2015; Klein et al., 2019). As *Cyp7b1* KO mice were impaired in their ability to maintain remote memory in the spatial memory task (Figures 2E and 2F), we examined whether *Cyp7b1* deficiency may affect the neuronal structural change in the hippocampus after the training of the Morris water maze task. The brains were isolated 6 hours after the last training and subjected to Golgi staining. Then, the brains were sliced into 100-μm-thick sections, and the dendritic spines were counted along dendrites of the Golgi-stained CA1 (Figure 3A) and DG neurons (Figure 3C) in trained or untrained mice (in detail, see Transparent Methods). In WT mice, the spine densities in basal dendrites of CA1 were significantly increased by the training (Figure 3B), as reported previously (Mahmmoud et al., 2015). *Cyp7b1* deficiency caused a decrease in the dendritic spine density in untrained mice when compared with untrained WT (Figure 3B). Importantly, *Cyp7b1* deficiency suppressed the training-dependent increase in the spine density (Figure 3B). Similarly, in the molecular layer of DG in WT mice, the spine densities were increased by the training (Figure 3D). We observed again that *Cyp7b1* deficiency caused a decrease in the spine density in untrained group and that, in *Cyp7b1* KO mice, the training induced no significant increase in the spine density (Figure 3D). These

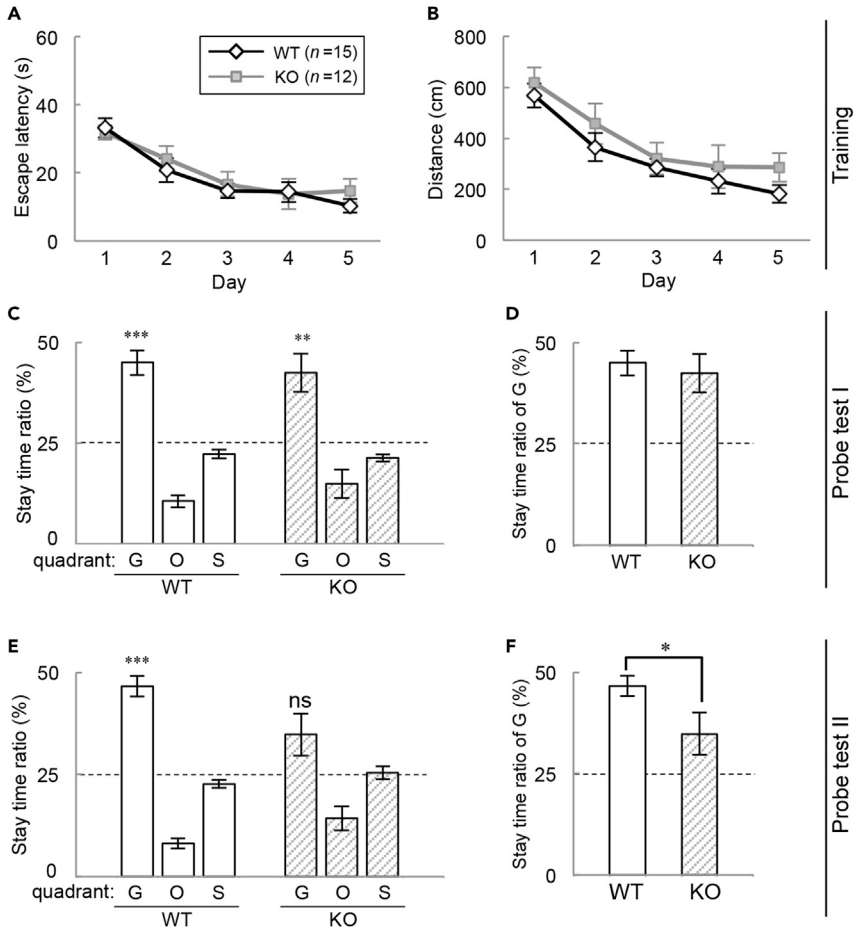

Figure 2. Spatial Memory Performance in Morris Water Maze Test of *Cyp7b1* KO Mice

(A–F) *Cyp7b1* KO and the littermate WT mice were subjected to the Morris water maze test. The training trials (4 trials/day) were performed for 5 consecutive days (Day 1–5). The escape latency to reach the hidden platform (A) and the swimming distance (B) on each day were averaged and plotted. Probe test I (Day 6) was performed on the next day of the last training (C and D). Probe test II was performed at 2 weeks after probe test I (E and F). In these probe tests, the hidden platform was removed, and stay time ratio in total of 60 s was calculated from the stay time in the goal (G) quadrant, the opposite (O) quadrant, or the side (S) quadrant (an average of right- and left-side quadrants was plotted) (C and E). Marks above the bars of the quadrant G indicate p values by Student's t test versus the chance level (25%). $^{**}p < 0.01$, $^{***}p < 0.001$, ns; not significant. (D and F) Stay time ratios in the quadrant G were compared between the two groups. $^{*}p = 0.0385$ by Student's t test. Values are shown as the mean ± SEM (WT, $n = 15$; KO, $n = 12$).

results suggest important roles of *Cyp7b1* in not only the training-dependent increase of the dendritic spines but also the generation and maintenance of the density in the hippocampus.

Detection of 7α-OH-Preg and 7α-OH-DHEA in the Hippocampus

The physiological phenotypes in *Cyp7b1* KO mice support important roles of 7α-OH-Preg and 7α-OH-DHEA, but these 7α-hydroxylated neurosteroids have not been detected in the rodent brain to date. In previous studies, trimethylsilyl-derivatized 7α-OH-Preg has been identified in the brain extracts of non-mammalian vertebrates by gas chromatography-mass spectrometric (MS) analysis (Matsunaga et al., 2004; Tsutsui et al., 2008; Hatori et al., 2011; Haraguchi et al., 2015). 7α-OH-DHEA was also identified in the ventricular cerebrospinal fluid of human as its trimethylsilyl derivative (Stárka et al., 2009). In liquid chromatography-tandem mass spectrometric (LC-MS/MS) analysis, on the other hand, many steroids were detected as multiply dehydrated forms (Mikšík et al., 2004), and the multiple dehydration hampered sensitive detection of 7α-OH-Preg and 7α-OH-DHEA. In the present study, we performed LC-MS/MS analysis without any derivatization of steroids by employing our recently developed procedure (Wang et al.,

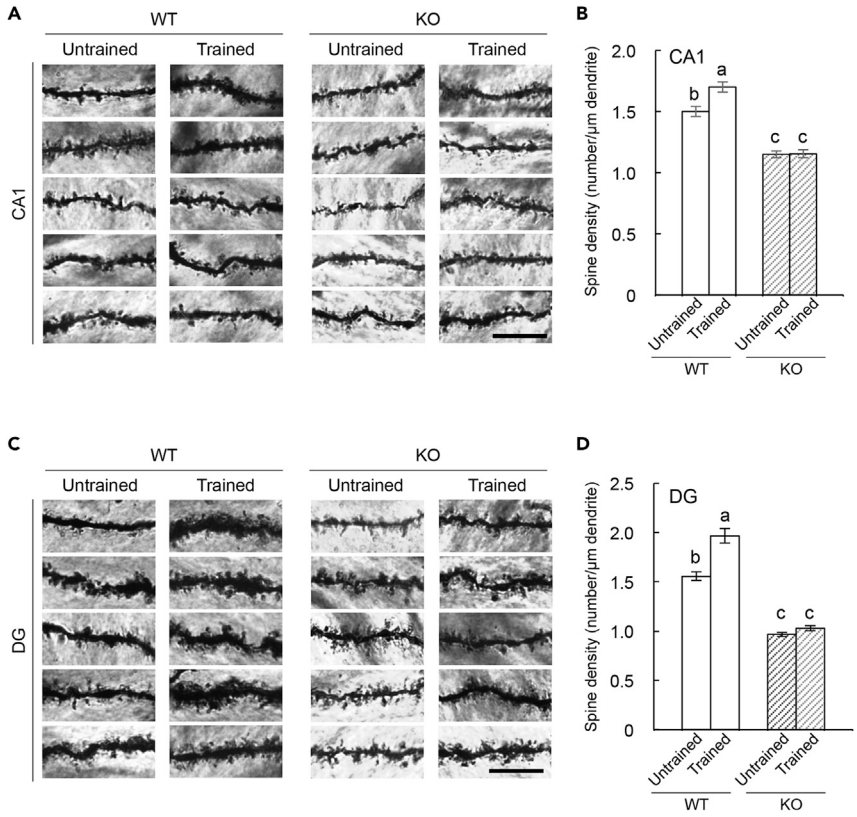

Figure 3. Training-Dependent Changes in Spine Density in the Hippocampus

(A) Representative images of spines on basal dendrites of Golgi-impregnated CA1 pyramidal cells. Scale bar, 10 μm.

(B) Spine density of basal dendrites of CA1 pyramidal cells. Tukey's test revealed a significant ($p < 0.05$) increase in spine density after Morris water maze (MWM) training in WT mice and a significantly low spine density in trained- and untrained-*Cyp7b1* KO mice compared with untrained-WT mice. Untrained-WT versus trained-WT, $p = 0.0010$; untrained-KO versus trained-KO, $p = 0.9999$; untrained-WT versus untrained-KO, $p < 0.0001$; untrained-WT versus trained-KO, $p < 0.0001$; trained-WT versus untrained-KO, $p < 0.0001$; trained-WT versus trained-KO, $p < 0.0001$.

(C) Representative images of spines on Golgi-impregnated DG granule cells. Scale bar, 10 μm.

(D) Spine density of dendrites of DG granule cells. Tukey's test revealed a significant ($p < 0.05$) increase in spine density after MWM training in WT mice and a significantly low spine density in trained- and untrained-*Cyp7b1* KO mice compared with untrained-WT mice. Untrained-WT versus trained-WT, $p < 0.0001$; untrained-KO versus trained-KO, $p = 0.7793$; untrained-WT versus untrained-KO, $p < 0.0001$; untrained-WT versus trained-KO, $p < 0.0001$; trained-WT versus untrained-KO, $p < 0.0001$; trained-WT versus trained-KO, $p < 0.0001$.

Values are shown as the mean ± SEM.

Distinct letters indicate statistical differences.

2020). Briefly, electrospray ionization (ESI) was performed with post-column addition of 0.1 mM (final concentration) lithium chloride to prevent multiple dehydration of the steroids. The selectivity and sensitivity in the MS detection were further enhanced by employing multiple reaction monitoring (MRM) mode. Therein, we set three major product ions (MRM transitions) for each authentic 7α-OH-Preg and 7α-OH-DHEA (Table S1), which were eluted at 5.90 min (Figure 4A) and 4.58 min (Figure 4D), respectively, in the LC. Each steroid gave a specific peak intensity ratio (Figure 4, inset) for the three MRM transitions. For compound identification, the peaks at each MRM transition should have the same retention time as those of each standard and their relative intensities should be in parallel with those of each standard. Then, 7α-OH-Preg and 7α-OH-DHEA were successfully identified in the mouse hippocampi isolated 2 h after the training trials on Day 1 (Figures 4C and 4F). In contrast, these neurosteroids were undetectable in the hippocampal extract prepared from naive (untrained) mice (Figures 4B and 4E). No significant peaks of these neurosteroids were detected in the hippocampal extracts prepared from *Cyp7b1* KO mice even after the training task (Figure S4), indicating that CYP7B1 is essential for biosyntheses of 7α-OH-Preg and 7α-OH-DHEA in the hippocampus. These observations in LC-MS/MS analysis, together with the impaired remote memory

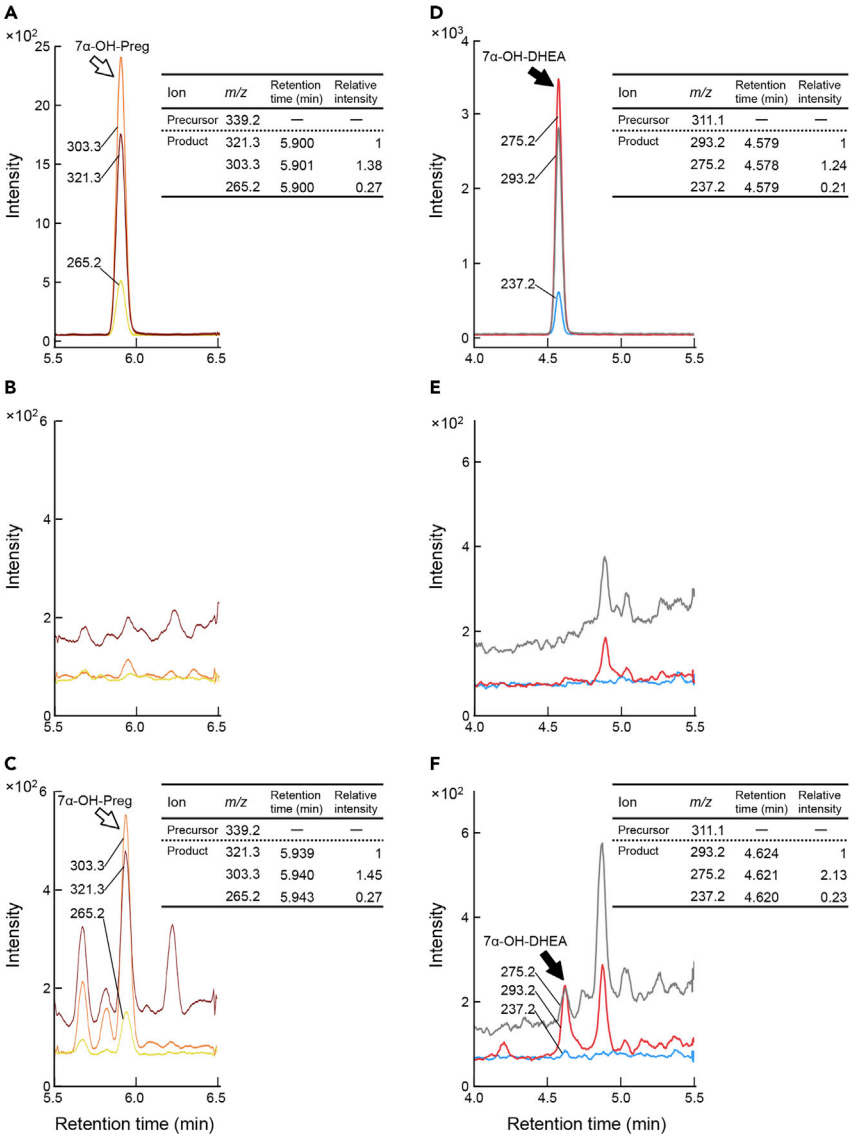

Figure 4. LC/ESI-MS/MS Analysis of 7α-OH-Preg and 7α-OH-DHEA in Mouse Hippocampal Extract

MRM chromatograms of LC-ESI-MS/MS analysis of standard 7α-OH-Preg (A) and 7α-OH-DHEA (D) solutions (100 pg each) and the hippocampal extract prepared from two naive mice (B and E) and two trained mice (C and F). The hippocampi were isolated from the mice 2 h after the one-day training (4 trials).

(A–C) MRM transitions for detecting 7α-OH-Preg were 339.2→321.3 (claret), 339.2→303.3 (orange), and 339.2→265.2 (yellow).

(D–F) MRM transitions for detecting 7α-OH-DHEA were 311.1→293.2 (gray), 311.1→275.2 (red), and 311.1→237.2 (blue). Relative peak intensities of these product ions are shown in the inset table.

performance in *Cyp7b1* KO mice (Figures 2E and 2F) and their decreased spine densities (Figure 3), suggest that training-induced 7α-OH-Preg and/or 7α-OH-DHEA in the hippocampus could be responsible for the spine remodeling and the formation of remote memory.

Rescue of Decreased Spine Density and Impaired Spatial Memory in *Cyp7b1* KO Mice by Chronic Infusion of 7α-Hydroxylated Steroids

We examined whether the abnormalities of the spine density and remote spatial memory due to *Cyp7b1* deficiency can be rescued by administration of 7α-OH-Preg and 7α-OH-DHEA. *Cyp7b1* KO mice were infused intracerebroventricularly with a mixture of 7α-OH-Preg and 7α-OH-DHEA (7αP+7αD; 455 ng/μL each) dissolved in

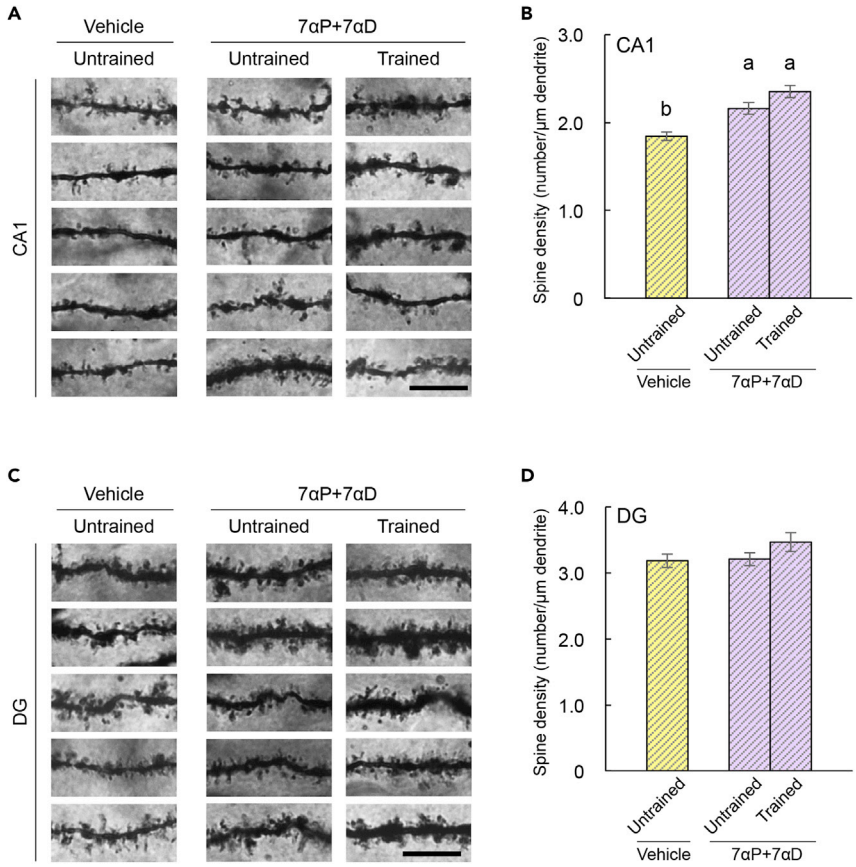

Figure 5. Effects of Infusion of Steroids into *Cyp7b1* KO Mice on Spine Density in the Hippocampus

(A) Representative images of spines on basal dendrites of Golgi-impregnated CA1 pyramidal cells. Scale bar, 10 μm.

(B) Spine density of basal dendrites of CA1 pyramidal cells. Tukey's test revealed a significant ($p < 0.05$) increase in spine density by infusion of a mixture of 7α-OH-Preg and 7α-OH-DHEA (7αP+7αD) to untrained and trained groups of KO mice when compared with vehicle-infused group. Vehicle (untrained) versus 7αP+7αD untrained, $p = 0.0008$; vehicle (untrained) versus 7αP+7αD trained, $p < 0.0001$; 7αP+7αD untrained versus 7αP+7αD trained, $p = 0.0988$.

(C) Representative images of spines on Golgi-impregnated DG granule cells. Scale bar, 10 μm.

(D) Spine density of dendrites of DG granule cells. Tukey's test revealed no significant difference in spine density among the three groups. Vehicle (untrained) versus 7αP+7αD untrained, $p = 0.9827$; vehicle (untrained) versus 7αP+7αD trained, $p = 0.2046$; 7αP+7αD untrained versus 7αP+7αD trained, $p = 0.2694$.

Values are shown as the mean ± SEM.

Distinct letters indicate statistical differences.

artificial cerebrospinal fluid (aCSF) containing 1% DMSO by using osmotic minipump (0.11 μL/h; 100 ng/h). As a control (vehicle), the aCSF containing 1% DMSO was infused into the KO mice. Three to five days after the infusion onset, some of the steroids-infused mice were subjected to the 5-days spatial-training trials (trained) and sacrificed 6 hours after the last trial, whereas the others were maintained in the home cage (untrained) and sacrificed at the same timing. The dendritic spine densities in the hippocampus were quantified as described for the dendritic spine analysis (Figure 3). The spine densities in basal dendrites of CA1 (Figure 5A) were significantly increased by the steroids infusion (Figure 5B; 7αP+7αD, untrained), when compared with the vehicle-infused control (vehicle, untrained). After the spatial-training task, no significant increase was observed in spine densities of the steroids-infused KO mice when compared with the steroids-infused untrained KO mice (Figure 5B; 7αP+7αD, trained). In the molecular layer of DG, on the other hand, there was no significant difference in spine densities among these three groups of the infused KO mice (Figures 5C and 5D). These steroids infused into the lateral ventricle may not have reached the DG.

We finally asked whether the impaired spatial memory of *Cyp7b1* KO mice is rescued by intracerebroventricular infusion of the 7α-hydroxylated steroids. *Cyp7b1* KO mice were divided into four groups, and the

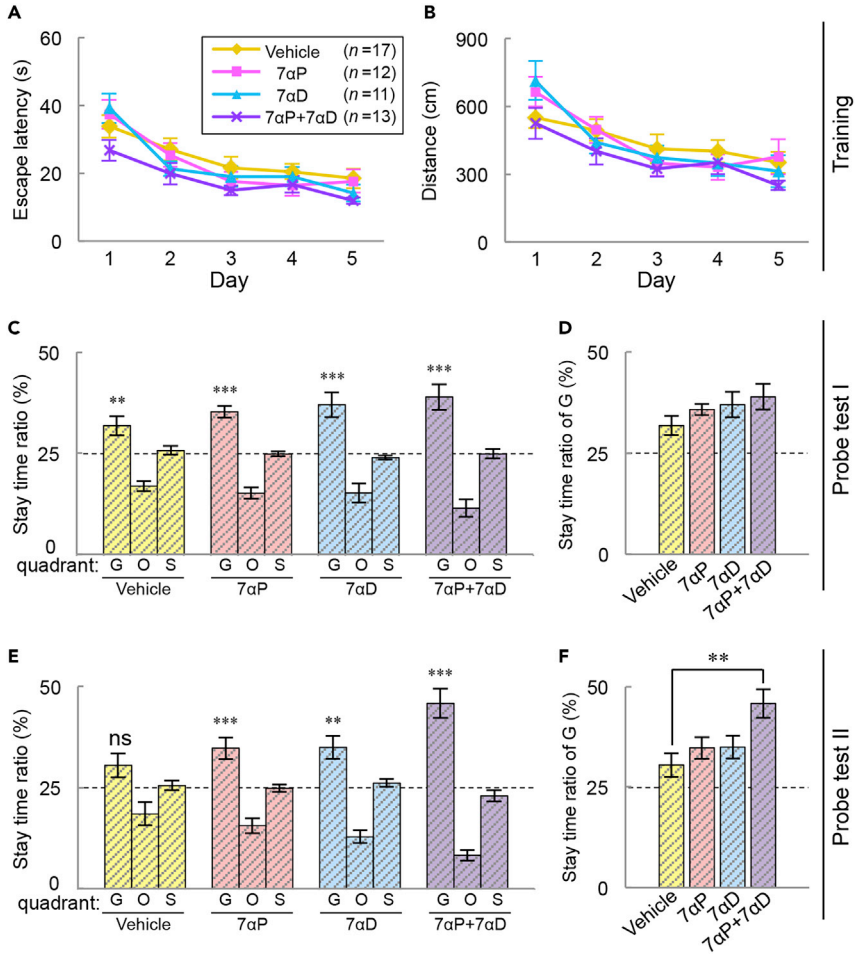

Figure 6. Effects of Infusion of Steroids into *Cyp7b1* KO Mice on Spatial Memory Performance in Morris Water Maze Test

(A–F) 7α-OH-Preg (7αP) and/or 7α-OH-DHEA (7αD) were infused into *Cyp7b1* KO mice intracerebroventricularly, and they were subjected to the Morris water maze test under the same condition with Figure 2 . (A) Average escape latency and (B) average swimming distance in the training. Probe test I (C and D) and probe test II (E and F) were performed. (C and E) Stay time ratio. Marks above the bars of quadrant G indicate p values by Student's t test versus the chance level (25%). **p < 0.01, ***p < 0.001, ns; not significant. (D and F) Stay time ratios in quadrant G **p = 0.0020 by Dunnett's test versus vehicle. Values are shown as the mean ± SEM (vehicle, *n* = 17; 7αP, *n* = 12; 7αD, *n* = 11; 7αP+7αD, *n* = 13).

mice were administered intracerebroventricularly with 7α-OH-Preg (910 ng/μL), 7α-OH-DHEA (910 ng/μL), a mixture of 7α-OH-Preg and 7α-OH-DHEA (455 ng/μL each), or vehicle (aCSF containing 1% DMSO) by using the osmotic minipump. Three to five days after the infusion onset, they were subjected to the Morris water maze task (Figure 6). In the training trials and the subsequent probe test I for recent memory, we found no significant difference among the four groups in not only the learning curves (Figures 6A and 6B) but also the stay time ratios in quadrant G (Figures 6C and 6D). The mice were then subjected to the probe test II 2 weeks later to examine remote memory performance. In vehicle-infused *Cyp7b1* KO mice, the stay time ratio in quadrant G was not significantly higher than the chance level (Figure 6E, vehicle), a phenotype that is almost similar to that seen in non-operated *Cyp7b1* KO mice (Figure 2E; KO). On the other hand, the KO mice infused with 7α-OH-Preg (7αP), 7α-OH-DHEA (7αD), and a mixture of 7α-OH-Preg and 7α-OH-DHEA (7αP+7αD) explored quadrant G significantly longer than the other quadrants (O and S) and their stay time ratios to quadrant G were significantly higher than the chance level (Figure 6E; 7αP, 7αD, and 7αP+7αD). Most strikingly, infusion of the mixture (7αP+7αD) into the KO mice remarkably enhanced the stay time ratio to quadrant G when compared with vehicle-infused KO mice (Figure 6F). It is noteworthy that remote spatial memory impaired by *Cyp7b1* deficiency was rescued significantly by administration of the mixture of 7α-hydroxylated steroids (455 ng/μL each) among the three treatments with the steroids

(910 ng/μL, in total). We conclude that 7α-OH-Preg and 7α-OH-DHEA cooperatively regulate the formation of remote spatial memory. The swimming distance and speed were unaffected by intracerebroventricular infusion of 7α-hydroxylated steroids in both probe tests (Figures S1E–S1H).

DISCUSSION

7α-OH-Preg was originally reported as a neurosteroid that stimulates locomotor activities of the newt (Matsunaga et al., 2004) and the quail (Tsutsui et al., 2008). Our previous results revealed the similar effect of intracerebroventricular injection of 7α-OH-Preg on the chick (Hatori et al., 2011). In the present study, however, *Cyp7b1* KO mice deficient in 7α-OH-Preg showed no obvious phenotype in daily locomotor activities under a light-dark cycle and constant darkness (Figure S2). Also, the swimming distance and the swimming speed were unaffected by either *Cyp7b1* deficiency or intracerebroventricular infusion of 7α-OH-Preg into the mutant mice (Figure S1). These results suggested that 7α-OH-Preg appears irrelevant to the regulation of locomotor activity of mice, and therefore the physiological function of 7α-OH-Preg in the brain would be different among species. We then paid attention to hippocampal function, because preceding studies detected high-level expression of *Cyp7b1* mRNA in the mouse DG (Rose et al., 2001) and 7α-hydroxylating activity (on DHEA) in the rat hippocampus (Yau et al., 2006). Indeed, we confirmed hippocampal mRNA expression of several genes required for the biosynthesis of 7α-OH-Preg and 7α-OH-DHEA (Figure 1).

In the hippocampus-dependent Morris water maze task, we found that only the retrieval (or retention) of spatial memory at the remote time point was impaired by *Cyp7b1* deficiency (Figures 2E and 2F). The impaired remote memory performance was partly rescued by single infusion of 7α-OH-Preg or 7α-OH-DHEA (Figure 6E; versus the chance level). We should emphasize that the remote memory performance of the KO mice was remarkably rescued by the mixture infusion of 7α-OH-Preg and 7α-OH-DHEA to a level comparable to that of WT mice (Figure 2F, WT and 6F, 7αP+7αD). Interestingly, co-infusion of these neurosteroids was more effective than the single infusion of each steroid, despite the concentrations of the singly administered steroids were the same with the total concentration of the mixture (Figure 6F). These results indicate that CYP7B1 plays a key role in a pathway important for long-term maintenance of spatial memory through the actions of 7α-OH-Preg and 7α-OH-DHEA and that these steroids function in a cooperative manner. We speculate that 7α-OH-Preg and 7α-OH-DHEA may have their individual targets of action for the retention of spatial memory. It is relevant to identify their targets for understanding how they regulate remote spatial memory. It is known that a decline of cognitive performance is associated with aging (Wahl et al., 2017). The recovery of the cognitive behavior by administration of the 7α-hydroxylated steroids (Figures 6E and 6F) suggests that aging may lead to a decline in biosynthesis of the 7α-hydroxylated steroids in the hippocampus.

The spine density analysis in the *Cyp7b1*-deficient hippocampus suggests that 7α-OH-Preg and 7α-OH-DHEA are involved in both maintenance of constitutive spine turnover and their training-dependent increase (Figure 3). Although the 7α-hydroxylated steroids were not detected in the hippocampal extract prepared from untrained WT mice (Figure 4), it is possible that the 7α-hydroxylated steroids are constantly present in the hippocampus at low levels (below detection limits of our LC-MS/MS analysis) and contribute to the maintenance of constitutive spine turnover in WT mice. During formation of declarative memory, hippocampal neurons undergo structural changes such as dendritic spine growth in the CA1 and DG (Leuner et al., 2003; Restivo et al., 2009; Mahmmoud et al., 2015). The dendritic spine density represents the number of hippocampal excitatory synapses (Leuner et al., 2003; Moser et al., 1994) and the density in CA1 neurons increases after spatial memory tasks (Moser et al., 1994; Eilam-Stock et al., 2012). We found that the intracerebroventricular infusion of 7α-OH-Preg and 7α-OH-DHEA rescued the phenotypes due to *Cyp7b1* deficiency, i.e., the decrease in the spine density in the CA1 (Figure 5) and the impairment of remote memory performance (Figures 6E and 6F). Our results together suggest that the training-induced neurosteroids elevate the CA1 spine density and that the process is essential for the formation of remote spatial memory. We think that the 7α-hydroxylated steroids may be associated with regulation of spine dynamics that is balanced between additions and eliminations of spines (Berry and Nedivi, 2017). Because the dendritic spine densities in the hippocampi of the untrained WT mice were significantly higher than those of the untrained KO mice (Figure 3), we speculate that the 7α-hydroxylated steroids may shift the balance to the additions and as a consequence increase the spine density. In the downstream of the neurosteroids actions, the spine density may be elevated by epigenetic transcriptional regulation (Kim et al., 2018) or enhancement of cAMP signaling (Lee et al., 2020).

Now, a question arises why were *Cyp7b1*-deficient mice able to retrieve spatial memory at the recent time point (Figure 2), even though their spine densities were unchanged after the training (Figure 3)? In the

previous articles (Leuner et al., 2003; Restivo et al., 2009; Mahmmoud et al., 2015; Cole et al., 2012), the spine density was correlated with behavioral expression of memory at the recent time. It is well established that the dendritic spines are heterogeneous in shape/function and that they are balanced dynamically (Mahmmoud et al., 2015; Berry and Nedivi, 2017). Although the spine densities in total were apparently unchanged after the training in the KO mice (Figure 3), it is possible that some spines important for retrieval of spatial memory at the recent time point may be enriched after the training. We face another question of why the infusion of the steroids did not restore the training-induced increase in the spine density (Figure 5B). One possibility is that the impaired memory retention was due to the reduced basal spine density. Rather, because the training enhanced the levels of neurosteroids (Figure 4), we speculate that the steroid infusion should have led the brain to a state after the training, and therefore, further training caused no significant increase in the dendritic spine density.

In parallel with the present study, we have developed a procedure for LC-MS/MS analysis of neurosteroids extracted from the mouse brain (Wang et al., 2020). By using the method with MRM analysis, we recently identified six neurosteroids in mouse whole brain extracts, in which 7α-OH-Preg and 7α-OH-DHEA were not detected (Wang et al., 2020). In the present study, the method was applied to the analysis of the hippocampal extract, and we eventually discovered the occurrence of 7α-OH-Preg and 7α-OH-DHEA in the hippocampus only after the spatial-learning task (Figures 4C and 4F). It is our future work to elucidate which step of neurosteroidogenesis is regulated by the training task and what element in the training task, e.g., learning or physical exercise, triggers the biosynthesis of these neurosteroids. The neurosteroidogenesis involves translocation of cholesterol to the mitochondria and between the mitochondrial membranes through the action(s) of rate-limiting enzymes such as StAR and other translocases (Selvaraj et al., 2018). Therefore, the translocation mechanism of cholesterol might be one of the keys to understanding the training-induced neurosteroidogenesis in the hippocampus. The possibility is not eliminated that the neurosteroids detected in the hippocampus are synthesized in other brain region(s) and transported to the hippocampus in a training-dependent manner. It is also possible that the training-induced 7α-hydroxylated steroids in the hippocampus may act on other brain region(s) such as anterior cingulate cortex for the long-term maintenance of spatial memory (Teixeira et al., 2006). Despite the possibilities, 7α-OH-Preg and 7α-OH-DHEA should be the key mediators for the spatial training-dependent increase in the spine density in hippocampal neurons, and these neurosteroids play an important role for the long-term maintenance of spatial memory in mice.

Limitations of the Study

We tried to quantify the levels of 7α-OH-Preg and 7α-OH-DHEA extracted from the whole hippocampus of a trained WT mouse. However, as the levels varied from individual to individual, we here demonstrated the training-dependent occurrence of the neurosteroids in the hippocampus.

Resource Availability

Lead Contact

Further information and requests should be directed to and will be fulfilled by the Lead Contact, Kimiko Shimizu (shimizuk@bs.s.u-tokyo.ac.jp).

Materials Availability

This study did not generate new unique reagents.

Data and Code Availability

All relevant data are available from the authors upon request.

METHODS

All methods can be found in the accompanying Transparent Methods supplemental file.

SUPPLEMENTAL INFORMATION

Supplemental Information can be found online at https://doi.org/10.1016/j.isci.2020.101559.

ACKNOWLEDGMENTS

We thank Ms. Yoriko Mawatari for excellent technical support. This work was performed in part under the Collaborative Research Program of Institute for Protein Research, Osaka University, CR-18-05. This work was supported by JSPS KAKENHI, Grant-in-Aid for Specially Promoted Research JP17H06096 to Y.F., Grant-in-Aid for Challenging Exploratory Research JP24657082 to K.S., and Grant Number JP16H06276 (AdAMS) to K.S.. T.I. is supported by JSPS fellowship (SPD).

AUTHOR CONTRIBUTIONS

K.M., K.S., and Y.F. designed the research, analyzed data, and wrote the main manuscript. K.M. prepared figures. K.M. performed real-time qPCR. K.M., K.S., and T.I. performed Morris water maze test of non-operated mice. K.S. and A.S. performed dendritic spine analysis of non-operated mice. K.M., K.S., Q.W., Y.P., and T.T. performed LC-MS/MS analysis. K.M. performed intracerebroventricular infusion of steroids, and Z.W. performed dendritic spine analysis of infused KO mice. K.M. and K.S. performed intracerebroventricular infusion of steroids and performed Morris water maze test of infused KO mice. K.M. analyzed locomotor activity and anxiety-like behavior. Y.F. supervised the research. All authors reviewed the manuscript.

DECLARATION OF INTERESTS

The authors declare no competing interests.

Received: July 6, 2020
Revised: August 1, 2020
Accepted: September 10, 2020
Published: October 23, 2020

REFERENCES

Akwa, Y., Morfin, R.F., Robel, P., and Baulieu, E.E. (1992). Neurosteroid metabolism. 7α-Hydroxylation of dehydroepiandrosterone and pregnenolone by rat brain microsomes. Biochem. J. *288*, 959–964.

Baulieu, É.É. (2000). 'New' active steroids and an unforeseen mechanism of action. C R Acad. Sci. III *323*, 513–518.

Berry, K.P., and Nedivi, E. (2017). Spine dynamics: are they all the same? Neuron *96*, 43–55.

Cole, C.J., Mercaldo, V., Restivo, L., Yiu, A.P., Sekeres, M.J., Han, J.-H., Vetere, G., Pekar, T., Ross, P.J., Neve, R.L., et al. (2012). MEF2 negatively regulates learning-induced structural plasticity and memory formation. Nat. Neurosci. *15*, 1255–1264.

Corpéchot, C., Robel, P., Axelson, M., Sjövall, J., and Baulieu, E.E. (1981). Characterization and measurement of dehydroepiandrosterone sulfate in rat brain. Proc. Natl. Acad. Sci. U S A *78*, 4704–4707.

Eilam-Stock, T., Serrano, P., Frankfurt, M., and Luine, V. (2012). Bisphenol-A impairs memory and reduces dendritic spine density in adult male rats. Behav. Neurosci. *126*, 175–185.

El Kihel, L. (2012). Oxidative metabolism of dehydroepiandrosterone (DHEA) and biologically active oxygenated metabolites of DHEA and epiandrosterone (EpiA)-recent reports. Steroids *77*, 10–26.

Haraguchi, S., Yamamoto, Y., Suzuki, Y., Chang, J.H., Koyama, T., Sato, M., Mita, M., Ueda, H., and Tsutsui, K. (2015). 7α-Hydroxypregnenolone, a key neuronal modulator of locomotion, stimulates upstream migration by means of the dopaminergic system in salmon. Sci. Rep. *5*, 12546.

Hatori, M., Hirota, T., Iitsuka, M., Kurabayashi, N., Haraguchi, S., Kokame, K., Sato, R., Nakai, A., Miyata, T., Tsutsui, K., et al. (2011). Light-dependent and circadian clock-regulated activation of sterol regulatory element-binding protein, X-box-binding protein 1, and heat shock factor pathways. Proc. Natl. Acad. Sci. U S A *108*, 4864–4869.

Kim, S., Yu, N.K., Shim, K.W., Kim, J.I., Kim, H., Han, D.H., Choi, J.E., Lee, S.W., Choi, D.I., Kim, M.W., et al. (2018). Remote memory and cortical synaptic plasticity require neuronal CCCTC-binding factor (CTCF). J. Neurosci. *38*, 5042–5052.

Klein, M.M., Cholvin, T., Cosquer, B., Salvadori, A., Le Mero, J., Kourouma, L., Boutillier, A.L., Pereira de Vasconcelos, A., and Cassel, J.C. (2019). Ventral midline thalamus lesion prevents persistence of new (learning-triggered) hippocampal spines, delayed neocortical spinogenesis, and spatial memory durability. Brain Struct. Funct. *224*, 1659–1676.

Lee, J., Lee, H.R., Kim, J.I., Baek, J., Jang, E.H., Lee, J., Kim, M., Lee, R.U., Kim, S., Park, P., and Kaang, B.K. (2020). Transient cAMP elevation during systems consolidation enhances remote contextual fear memory. Neurobiol. Learn. Mem. *169*, 107171.

Leuner, B., Falduto, J., and Shors, T.J. (2003). Associative memory formation increases the observation of dendritic spines in the hippocampus. J. Neurosci. *23*, 659–665.

Li-Hawkins, J., Lund, E.G., Turley, S.D., and Russell, D.W. (2000). Disruption of the oxysterol 7α-hydroxylase gene in mice. J. Biol. Chem. *275*, 16536–16542.

Mahmmoud, R.R., Sase, S., Aher, Y.D., Sase, A., Gröger, M., Mokhtar, M., Höger, H., and Lubec, G. (2015). Spatial and working memory is linked to spine density and mushroom spines. PLoS One *10*, e0139739.

Matsunaga, M., Ukena, K., Baulieu, E.-E., and Tsutsui, K. (2004). 7α-Hydroxypregnenolone acts as a neuronal activator to stimulate locomotor activity of breeding newts by means of the dopaminergic system. Proc. Natl. Acad. Sci. U S A *101*, 17282–17287.

Mikšík, I., Mikulíková, K., Pácha, J., Kučka, M., and Deyl, Z. (2004). Application of liquid chromatography – electrospray ionization mass spectrometry for study of steroid-converting enzymes. J. Chromatogr. B Analyt. Technol. Biomed. Life Sci. *800*, 145–153.

Morfin, R.F., and Courchay, G. (1994). Pregnenolone and dehydroepiandrosterone as precursors of native 7-hydroxylated metabolites which increase the immune response in mice. J. Steroid Biochem. Mol. Biol. *50*, 91–100.

Moser, M.B., Trommald, M., and Andersen, P. (1994). An increase in dendritic spine density on hippocampal CA1 pyramidal cells following spatial learning in adult rats suggests the formation of new synapses. Proc. Natl. Acad. Sci. U S A *91*, 12673–12675.

Payne, A.H., and Hales, D.B. (2004). Overview of steroidogenic enzymes in the pathway from cholesterol to active steroid hormones. Endocr. Rev. *25*, 947–970.

Pringle, A.K., Schmidt, W., Deans, J.K., Wulfert, E., Reymann, K.G., and Sundstrom, L.E. (2003). 7-Hydroxylated epiandrosterone (7-OH-EPIA) reduces ischaemia-induced neuronal damage both in vivo and in vitro. Eur. J. Neurosci. *18*, 117–124.

Restivo, L., Vetere, G., Bontempi, B., and Ammassari-Teule, M. (2009). The formation of recent and remote memory is associated with time-dependent formation of dendritic spines in the hippocampus and anterior cingulate cortex. J. Neurosci. *29*, 8206–8214.

Rose, K.A., Stapleton, G., Dott, K., Kieny, M.-P., Best, R., Schwarz, M., Russell, D.W., Björkhem, I., Seckl, J.R., and Lathe, R. (1997). Cyp7b, a novel brain cytochrome P450, catalyzes the synthesis of neurosteroids 7α-hydroxy dehydroepiandrosterone and 7α-hydroxy pregnenolone. Proc. Natl. Acad. Sci. U S A *94*, 4925–4930.

Rose, K.A., Allan, A., Gauldie, S., Stapleton, G., Dobbie, L., Dott, K., Martin, C., Wang, L., Hedlund, E., Seckl, J.R., et al. (2001). Neurosteroid hydroxylase CYP7B: vivid reporter activity in dentate gyrus of gene-targeted mice and abolition of a widespread pathway of steroid and oxysterol hydroxylation. J. Biol. Chem. *276*, 23937–23944.

Selvaraj, V., Stocco, D.M., and Clark, B.J. (2018). Current knowledge on the acute regulation of steroidogenesis. Biol. Reprod. *99*, 13–26.

Stárka, L., Hill, M., Kancheva, R., Novak, Z., Chrastina, J., Pohanka, M., and Morfin, R. (2009). 7-Hydroxylated derivatives of dehydroepiandrosterone in the human ventricular cerebrospinal fluid. Neuroendocrinol. Lett. *30*, 368–372.

Teixeira, C.M., Pomedli, S.R., Maei, H.R., Kee, N., and Frankland, P.W. (2006). Involvement of the anterior cingulate cortex in the expression of remote spatial memory. J. Neurosci. *26*, 7555–7564.

Tsutsui, K., Inoue, K., Miyabara, H., Suzuki, S., Ogura, Y., and Haraguchi, S. (2008). 7α-hydroxypregnenolone mediates melatonin action underlying diurnal locomotor rhythms. J. Neurosci. *28*, 2158–2167.

Tsutsui, K., Haraguchi, S., Hatori, M., Hirota, T., and Fukada, Y. (2013). Biosynthesis and biological actions of pineal neurosteroids in domestic birds. Neuroendocrinology *98*, 97–105.

Wahl, D., Coogan, S.C.P., Solon-Biet, S.M., De Cabo, R., Haran, J.B., Raubenheimer, D., Cogger, V.C., Mattson, M.P., Simpson, S.J., and Le Couteur, D.G. (2017). Cognitive and behavioral evaluation of nutritional interventions in rodent models of brain aging and dementia. Clin. Interv. Aging *12*, 1419–1428.

Wang, Q.Y., Shimizu, K., Maehata, K., Pan, Y., Sakurai, K., Hikida, T., Fukada, Y., and Takao, T. (2020). Lithium ion adduction enables UPLC-MS/MS-based analysis of multi-class, 3-hydroxyl group-containing keto-steroids. J. Lipid Res. *61*, 570–579.

Wingfield, J.C., Wacker, D.W., Bentley, G.E., and Tsutsui, K. (2018). Brain-derived steroids, behavior and endocrine conflicts across life history stages in birds: a perspective. Front. Endocrinol. (Lausanne). *9*, 270.

Yau, J.L.W., Rasmuson, S., Andrew, R., Graham, M., Noble, J., Olsson, T., Fuchs, E., Lathe, R., and Seckl, J.R. (2003). Dehydroepiandrosterone 7-hydroxylase cyp7b: predominant expression in primate hippocampus and reduced expression in Alzheimer's disease. Neuroscience *121*, 307–314.

Yau, J.L.W., Noble, J., Graham, M., and Seckl, J.R. (2006). Central administration of a cytochrome P450-7B product 7α-hydroxypregnenolone improves spatial memory retention in cognitively impaired aged rats. J. Neurosci. *26*, 11034–11040.

iScience, Volume *23*

Supplemental Information

Hippocampal 7α-Hydroxylated Neurosteroids Are Raised by Training and Bolster Remote Spatial Memory with Increase of the Spine Densities

Kanako Maehata, Kimiko Shimizu, Tomoko Ikeno, Qiuyi Wang, Ayaka Sakurai, Zefeng Wei, Yue Pan, Toshifumi Takao, and Yoshitaka Fukada

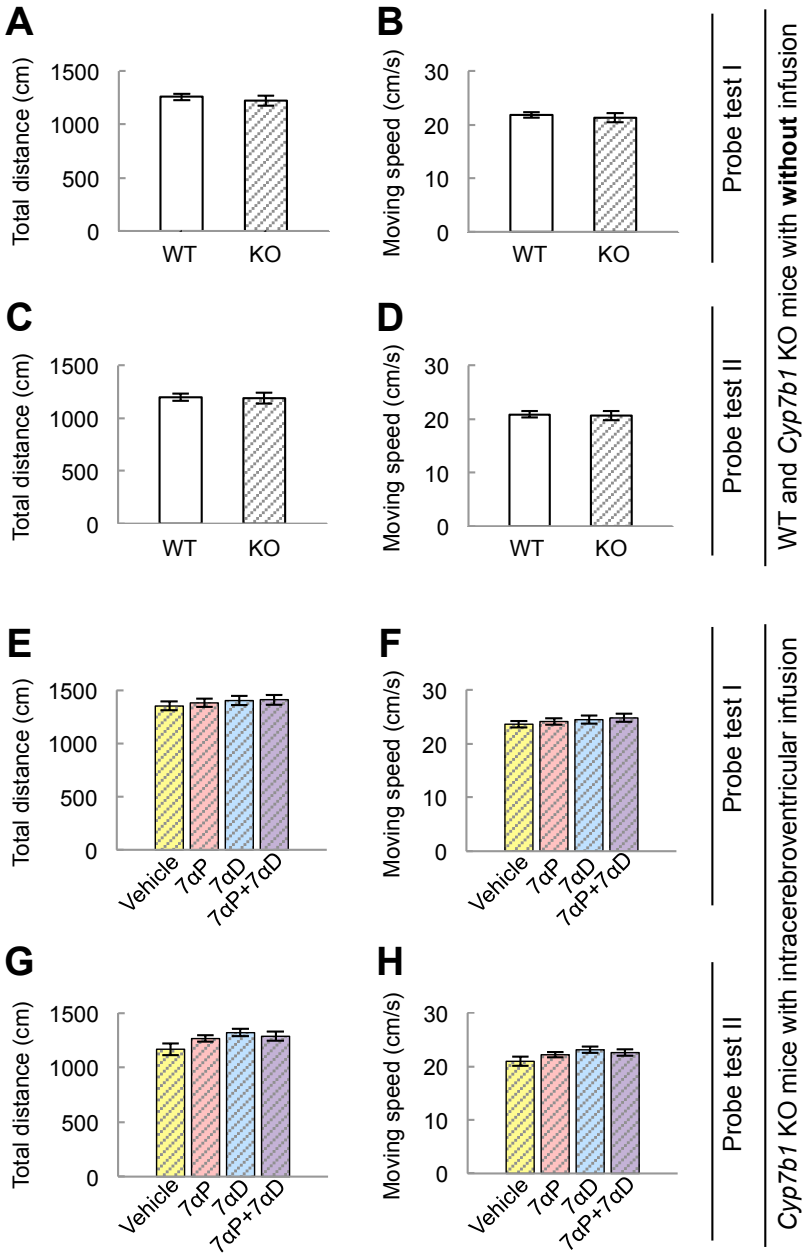

Figure S1. Activity parameters in probe tests of the Morris water maze test. Related to Figure 2 and Figure 6.

Total distance (**A**, **C**, **E**, **G**) and moving speed (**B**, **D**, **F**, **H**) of mice in the probe tests of the Morris water maze test (Fig 2, 6). Activities of (**A**, **B**) probe test I and (**C**, **D**) probe test II for *Cyp7b1* KO and the littermate WT mice in Fig 2. Not significant (P>0.05) by Student's t test. Activities of (**E**, **F**) probe test I and (**G**, **H**) probe test II for *Cyp7b1* KO mice with intracerebroventricular infusion of steroids in Fig 6. Not significant (P>0.05) by Dunnett's test *versus* vehicle. Values are shown as the mean ± SEM.

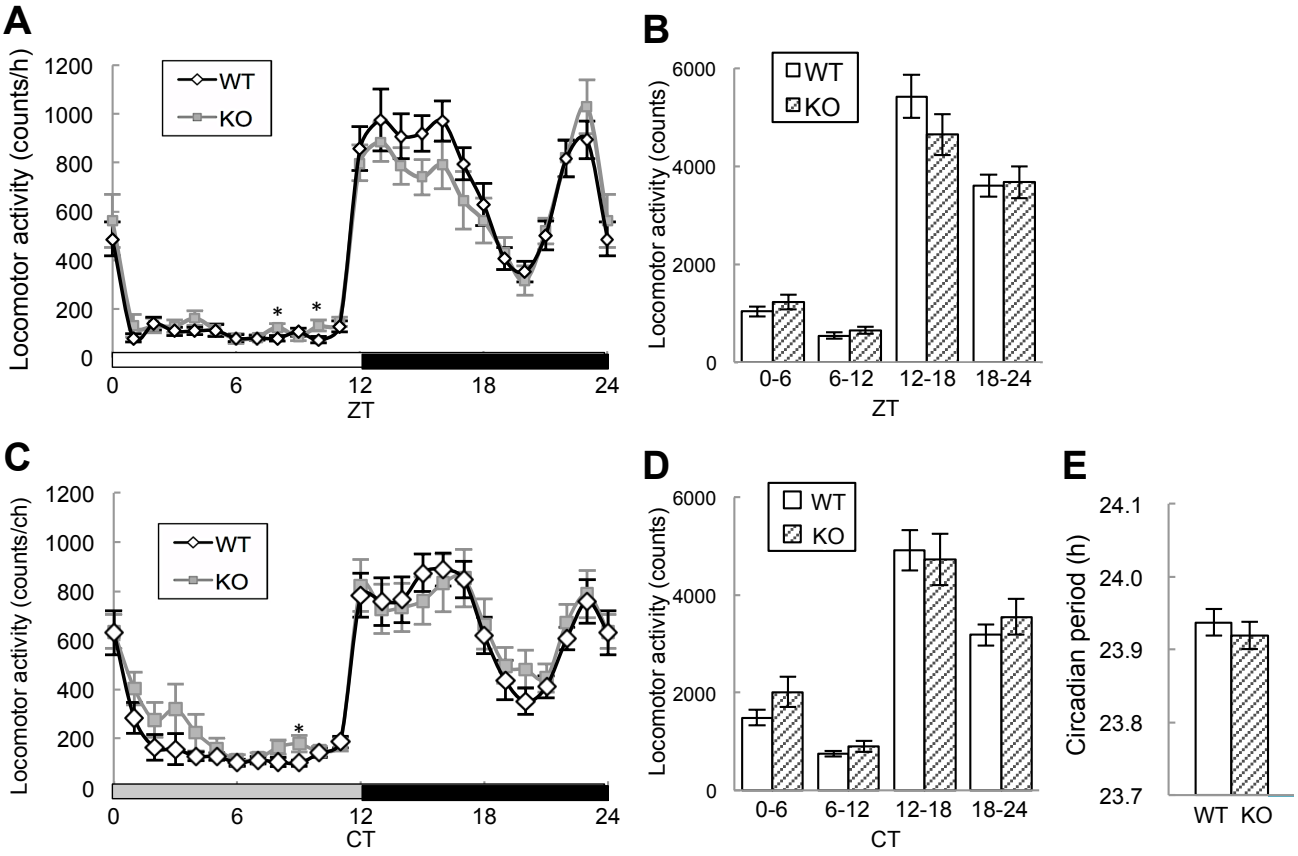

Figure S2. Locomotor activities and circadian periods of *Cyp7b1* KO mice and the littermate WT mice. Related to Figure 2.

Cyp7b1 KO and the littermate WT mice were entrained to a 12 hr/12 hr light/dark cycle (LD) and transferred to constant darkness (DD). Their free moving locomotor activities were monitored using infrared area sensors. (**A**) Averaged locomotor activities in LD (counts in one hour) were plotted against zeitgeber time (ZT). (**B**) Averaged locomotor activities in LD (counts in six hours) during the four time zones (ZT0-6, 6-12, 12-18, 18-24). (**C**) Averaged locomotor activities in DD (counts in one circadian hour) were plotted against circadian time (CT). (**D**) Averaged locomotor activities in DD (counts in six circadian hours) during the four time zones (CT0-6, 6-12, 12-18, 18-24). (**E**) Circadian periods in DD. In A-E, values are calculated from the activities in 14 days for each mouse and shown as the mean ± SEM (WT, n = 15; KO, n = 14). $^{*}P<0.05$ by Student's t test.

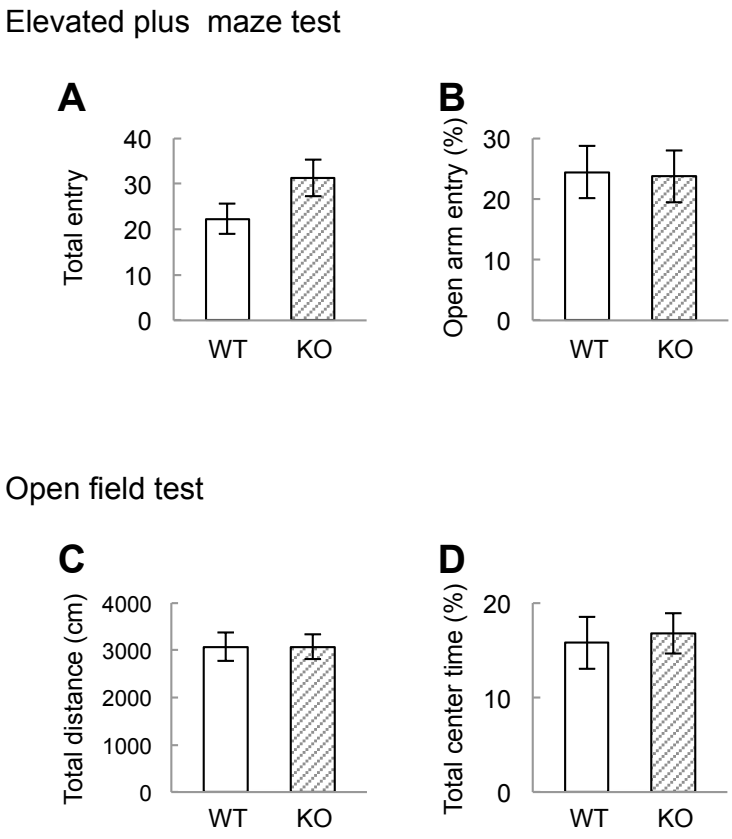

Figure S3. Anxiety-like behavior of *Cyp7b1* KO mice. Related to Figure 2.

Cyp7b1 KO and the littermate WT mice were subjected to elevated plus maze (EPM) test and open field (OF) test. Each mouse was subjected to both or one of these behavioral tests in the following order at least every second day. EPM test: (**A**) number of total arm entries and (**B**) ratio of number of open arm entries (WT, $n = 16$; KO, $n = 10$). OF test: (**C**) total distance explored for OF and (**D**) time ratio spent in center area (WT, $n = 12$; KO, $n = 11$). Values are shown as the mean ± SEM. Not significant ($P>0.05$) by Student's t test.

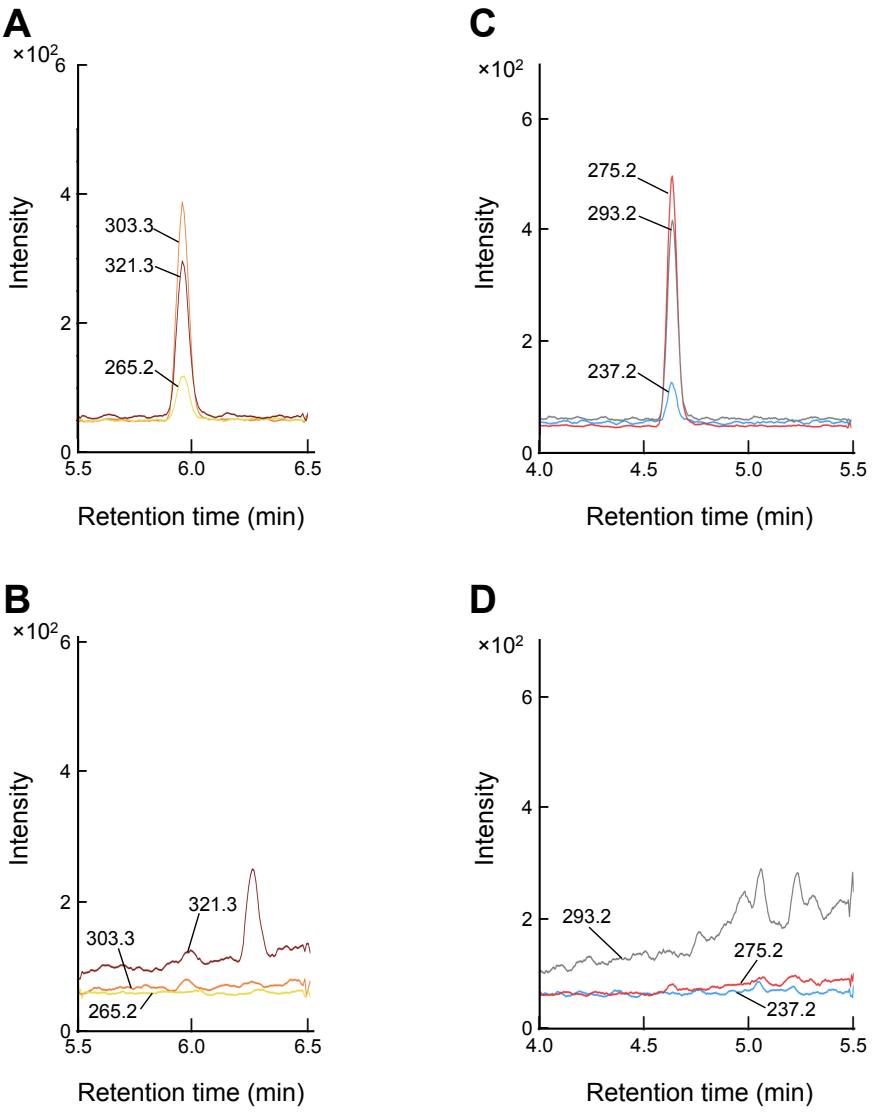

Figure S4. LC/ESI-MS/MS analysis of 7α-OH-Preg and 7α-OH-DHEA in the hippocampal extract of trained KO mice. Related to Figure 4.

MRM chromatograms of LC-ESI-MS/MS analysis of standard 7α-OH-Preg (**A**) and 7α-OH-DHEA (**C**) solutions (10 pg each) and the hippocampal extract in trained KO mice (**B**, **D**). (**A**, **B**) MRM transitions for detecting 7α-OH-Preg were 339.2->321.3 (claret), 339.2->303.3 (orange), and 339.2->265.2 (yellow). (**C**, **D**) MRM transitions for detecting 7α-OH-DHEA were 311.1->293.2 (gray), 311.1->275.2 (red), and 311.1->237.2 (blue).

Supplemental table

Table S1. Product ion species of 7α-OH-Preg and 7α-OH-DHEA employed in multiple reaction monitoring (MRM) analysis of UPLC/ESI-MS/MS. Related to Figure 4.

Compound Name	RT/ min	Precursor Ion	MS1 Res	Product Ion	MS2 Res	Dwell	Fragmentor	Collision Energy	Cell Accelerator Voltage
7α-OH-Preg	5.900	339.2	Widest	321.3	Unit	20	155	18	4
	5.901			303.3				20	
	5.900			265.2				24	
7α-OH-DHEA	4.579	311.1	Widest	293.2	Unit	20	155	19	4
	4.578			275.2				20	
	4.579			237.2				24	

Transparent Methods

Animals

Male mice (11-18 weeks) were housed under a 12 hr/12 hr light/dark cycle (LD) with the light provided by a white fluorescent lamp (300-400 lx at the level of the heads of mice) in a light-tight chamber at 23 ± 1 °C and constant humidity (55 ± 10 %) in cages with commercial chow (CLEA Japan, Inc.) and water available *ad libitum*. The time point when the light turned on was defined as zeitgeber time (ZT) 0 and the turned off as ZT12. In all the behavioral experiments, mice were housed individually in their home cages, and handled daily for at least one week before the tasks. All animal experiments described here adhered to local guidelines of the University of Tokyo, and all appropriate ethical approval and licenses were obtained.

Cyp7b1 knockout mice on the C57BL/6J genetic background were obtained from the Jackson Laboratory. In this mutant, deletion of exon 6 of the *Cyp7b1* gene eliminated CYP7B1 protein and its enzyme activity completely (Li-Hawkins *et al.*, 2000). Previously, it was reported that *Cyp7b1* KO mice have defects in prostate proliferation (Omoto *et al.*, 2005) or reproductive behaviors (Oyola *et al.*, 2015), but in our laboratory, *Cyp7b1* KO mice were fertile and apparently indistinguishable from WT mice in terms of survival and gross physical appearances as described by Li-Hawkins *et al*. (Li-Hawkins *et al.*, 2000).

To investigate locomotor activity, mice were housed individually in cages equipped with infrared area sensors (Elekit). Mice were entrained to a light/dark (LD) cycle for at least four weeks and released into constant darkness (DD). The total activities were recorded in five-min bins and analyzed with ClockLab analysis software (Actimetrics). The circadian period of the activity rhythms in DD was determined by using an extrapolation procedure with ClockLab. The time points of the onsets of mice activity were defined as circadian time (CT) 12.

RNA extraction and RT-qPCR

Total RNAs were extracted from the mouse brain regions by TRIzol reagent (Invitrogen). Total RNAs extracted from the pineal glands and the prefrontal cortexes were purified by using RNeasy MinElute Cleanup Kit (Qiagen), and those from the other brain tissues were purified by using RNeasy Mini Kit (Qiagen) according to the manufacturer's protocol. The RNAs were reverse-transcribed into cDNA using oligo $(dT)_{15}$ primer with GoScript Reverse Transcriptase (Promega). The cDNA was subjected to quantitative PCR using GoTaq qPCR Master Mix (Promega) with the StepOnePlus Real-time PCR system (Applied Biosystems) according to the manufacturer's protocol. The mRNA levels were quantified using a relative standard curve

method with hippocampal cDNAs as the standard. The gene-specific primers used for RT-qPCR were *StAR*-Fw (5'-GCTGG AAGCT CCTAT AGACA-3'), *StAR*-Rv (5'-AGCTC CGACG TCGAA CTTGA-3'), *Cyp11a1*-Fw (5'-ACATG GCCAA GATGG TACAG TTG-3'), *Cyp11a1*-Rv (5'-ACGAA GCACC AGGTC ATTCA C-3'), *Cyp7b1*-Fw (5'-CGGAA ATCTT CGATG CTCC-3'), *Cyp7b1*-Rv (5'-TAGCC CTATA GGCTT CCTGT CG-3'), *Cyp17a1*-Fw (5'-TGACC AGTAT GTAGG CTTCA GTCG-3'), *Cyp17a1*-Rv (5'-TCCTT CGGGA TGGCA AACTC TC-3'), *Rps29*-Fw (5'-TGAAG GCAAG ATGGG TCAC-3'), and *Rps29*-Rv (5'-GCACA TGTTC AGCCC GTATT-3').

Morris water maze test

The Morris water maze test was performed in a white Plexiglas circular pool (30 × ϕ100 cm; O'Hara & Co., Tokyo, Japan), which was set at a fixed position apart from the room walls and curtains and filled to a depth of 21 cm with 24 ± 1 °C water made opaque by adding TiO_2 (3 g). A circular escape platform (20 cm height, ϕ10 cm) was placed 1 cm below the water surface at a fixed position in a goal quadrant. All the experiments were performed under a flat white LED light at 4.0 ± 0.1 lx at the water surface. For the purpose of habituation to the platform before the water maze training, a mouse was placed on the platform surrounded by an equilateral triangle frame (40 cm on a side, 45 cm in height) without any visible cues and kept there for three min.

Male mice (11-18 weeks) of *Cyp7b1* KO and the littermate WT were composed of 12-15 individuals. The mice were trained for five consecutive days (Day 1 to Day 5) at ZT1 with four training trials per day at three to seven min inter-trial intervals. On each training trial, a start position was selected randomly from one of the three positions at the pool edge of the quadrants (right, left, and opposite to the goal quadrant). The mouse was gently placed in the water facing the wall. The trial was completed once the mouse found the hidden platform. If the mouse failed to reach the platform within 60 sec on a given trial, an experimenter gently guided the mouse onto the platform.

On the next day (Day 6) of the last training, spatial memory was assessed by a probe test (probe test I), in which the platform was removed from the pool. The mouse was allowed to search for the platform for 60 sec, and the time when the mouse stayed in each quadrant was measured. A similar probe test (probe test II) was performed at two weeks after the probe test I.

All the mouse behaviors were recorded by a video camera positioned right above the pool. The trace and the swimming speed were analyzed by a computer-operated system (TimeMWM;

O'Hara & Co., Tokyo, Japan), which also judged the goal time (escape latency) by detecting two-sec stay time on the platform. Rate of the recording was 25 frames/sec.

Golgi staining and dendritic spine analysis

Mice were trained in the Morris water maze task (trained) or maintained without training (untrained). Brains were isolated six hours after the last training and stained by using FD Rapid GolgiStain kit (FD NeuroTechnologies, Inc) according to the manufacturer's protocol. Briefly, the brains were rinsed with water and immersed in a mixture of FD Solution A/B (1/1, v/v, 2 mL) overnight at room temperature in the dark. On the next day, the mixed solution was renewed and brains were incubated at room temperature in the dark for two weeks. Then, brains were transferred to 2 mL FD Solution C. On the next day, the solution was renewed and brains were further incubated at room temperature in the dark for one week. The solution was removed and the brains were frozen at -80 °C. The cryoprotected brains were sliced into 100 μm-thick sections using a microtome-cryostat (Leica). Sections were put on 3% gelatin-coated slides and dried overnight before staining. The sections were rinsed twice with chilled water and immersed in a mixture of FD Solution D/E/water (1/1/2, v/v/v, 200 mL) for 10 min. After rinse twice with chilled water, sections were dehydrated in a series of ethanol solutions (50%, 75%, 95%, and 100% ethanols).

Dendrites spanning from hippocampal neurons of both hemispheres were drawn using a camera lucida attached to a Leica DMI6000B microscope (magnification 100×). The images were analyzed by using Neurolucida software (MBF Bioscience). In hippocampal CA1, regions between the first through second-order branches (12- to 100-μm length) of the dendrites located at 20- to 150-μm distances from the center of the cell body were traced and the dendritic spines were counted. Totally three basal dendrites per single neuron were selected from each mouse (n = 5; 12 neurons per each mouse). In the molecular layer of DG, regions between the first through second-order branches (17- to 300-μm length) of the dendrites located at 30- to 200-μm distances from the center of the cell body were traced and the spines were counted. Totally three dendrites per single neuron were selected from each mouse (n = 5; 12 neurons per each mouse). The spine densities (number per 1 μm) were averaged across animals in each group.

Extraction and purification of steroids

Mice were trained in the Morris water maze task (first day only, 4 trials), and sacrificed two hours after the last trial. Hippocampi isolated from two male mice were homogenized in ten

volumes (0.6 mL) of 0.25 M acetic acid solution with a glass-Teflon homogenizer on ice. Steroids were extracted by 0.6 mL ethyl acetate three times, and the extracts collected in glassware were evaporated under a gentle stream of nitrogen. The dried extract was dissolved in 0.75 mL acetonitrile/H_2O (50/50, v/v), collected in a 1.5 mL-tube and then centrifuged (3,000 × *g*, 5 min, 4 °C). The supernatant was diluted with 0.75 mL H_2O and subjected to purification with a solid-phase extraction column (HF Bond Elut, 50 mg, 1 mL; Agilent), which had been pre-washed two times with 0.5 mL acetonitrile/H_2O (80/20, v/v) and equilibrated with 1 mL acetonitrile/H_2O (5/95, v/v) successively. The sample was loaded on the column and the flow-through fraction was discarded. The column was then washed three times with 0.5 mL acetonitrile/H_2O (5/95, v/v), and the steroid fraction was eluted with 0.5 mL acetonitrile/H_2O (80/20, v/v) and evaporated under vacuum.

Liquid chromatography-mass spectrometry

7α-OH-Preg and 7α-OH-DHEA were separated by using an Agilent 1290 Infinity II LC system (Waldbronn, Germany) consisting of a binary pump, a micro vacuum degasser, a temperature controlled auto-sampler and a column oven. The sample storage temperature was 4 °C. The stationary phase was an Agilent Eclipse Plus C18 RRHD column (2.1×100 mm, particle size: 1.8 μm), which was maintained at 40 °C. The steroid sample was dissolved in methanol/H_2O (40/60, v/v; 12 μL), and 10 μL of the reconstituted sample was injected and eluted at a flow rate of 0.4 mL/min. The mobile phase consisted of 0.1% formic acid in H_2O (solvent A) and 0.1% formic acid in methanol (solvent B). The elution gradient was formed as follows: 40-80% B from 0 to 8 min, 80% B from 8 to 10 min, 80-40% from 10.0 to 10.1 min, and 40% B from 10.1 to 13.1 min. The post-column addition of 0.2 mM LiCl (final 0.1 mM) was done with Agilent 1100 binary pump as the auxiliary pump. Mass spectrometry experiments were performed with electrospray ionization (ESI) in positive ion mode. The capillary voltage was -3,500 V. The gas temperature was maintained at 210 °C. The sheath gas temperature was 275 °C and the flow rate was 12 L/min. The nebulizer gas flow was 13 L/min. Multiple reaction monitoring (MRM) was applied for highly selective and sensitive detection of 7α-OH-Preg and 7α-OH-DHEA. Three different MRM transitions were set and the measuring condition was optimized for each steroid as shown in Table S1. It was difficult to quantify small amounts of the steroids in the hippocampal extract due to noisy baseline (Figure 4C, F).

Intracerebroventricular infusion of steroids

Cyp7b1 KO male mice (11-15 weeks) were anesthetized by an intraperitoneal injection (20 μL/g body weight) of a mixture of ketamine (4.4 mg/mL; Daiichi Sankyo Propharma) and xylazine (0.44 mg/mL; Bayer Health Care) dissolved in bacteriostatic saline. The anaesthetized animals were placed in a stereotaxic frame (Narishige Inc.) keeping bregma and lambda at a horizontal level. A small hole was drilled in the skull, and a chronic indwelling stainless-steel cannula (ALZET Brain Infusion Kit 1; DURECT Co.) was placed into the right lateral ventricle using the following coordinates relative to bregma: 0.22 mm posterior; 1.0 mm right lateral; 2.3 mm below the horizontal plane of bregma. The cannula was fixed to the skull with adhesive and dental cement, and the external part of the intracerebroventricular cannula was connected with polyethylene tube to an ALZET osmotic minipump with an infusion rate of 0.11 μL/h for four weeks (model 1004; DURECT Co.) placed subcutaneously on the back. Steroids were dissolved in an artificial cerebrospinal fluid (aCSF) containing 1% DMSO. aCSF was prepared by mixing the same volume of solvent A containing 150 mM NaCl, 3 mM KCl, 1.4 mM $CaCl_2$, 0.8 mM $MgCl_2$ and solvent B containing 0.8 mM Na_2HPO_4, 0.2 mM NaH_2PO_4, and pH was adjusted at 7.4 with NaOH. The concentration of 7α-OH-Preg (Steraloids Inc.) or 7α-OH-DHEA (Steraloids Inc.) solution was 910 ng/μL, and that of the mixed steroid solution was 455 ng/μL each of 7α-OH-Preg and 7α-OH-DHEA. The dose of steroids was chosen based on the previous study (Yau *et al.*, 2006). All the mice were handled for at least one week before the surgery, housed individually after the surgery and allowed to recover at least three days before the Morris water maze test.

Elevated plus maze test

The elevated plus maze (EPM) was constructed of Plexiglas (O'Hara & Co., Tokyo, Japan) with two open arms (25×5 cm) and two enclosed arms with clear walls (15 cm height) at an elevation of 50 cm above the floor. The arms of the maze form a cross with the two open arms facing each other. The maze was washed and dried after each test.

Male mice of *Cyp7b1* KO and the littermate WT were composed of 10-16 individuals. The mice were placed on the center of the maze alone facing one of the closed arms under a flat white LED light at 4.0 lx ± 0.1 lx at the center of the apparatus. The behavior was recorded for 5 min by a video camera positioned above the maze. The rate of recording: 4 frame/s, moving criterion: 3 cm.

The numbers of entries into the open and closed arms and the time spent exploring the open and closed arms were analyzed using a computer-operated system (TimeEP1; O'Hara & Co., Tokyo, Japan).

Open field test

Male mice of *Cyp7b1* KO and the littermate WT were composed of 11-12 individuals. The mice were placed alone in the right front corner of a white Plexiglas open field arena (40×40 cm, 30 cm height) (O'Hara & Co., Tokyo, Japan) and allowed to explore for 5 min under a white LED light at 330 lx ± 10 lx at the center of the apparatus. The arena was cleaned up with disinfectant spray and water spray in this order after each test. The activity in the open field was recorded by a video camera positioned above the arena using a computer-operated system (OpenField plug-in; O'Hara & Co., Ltd.), a modified software based on the public domain Image J program (developed at the U.S. National Institutes of Health and available on the Internet at http://rsb.info.nih.gov/ij). Total distance and the time spent in the center area of the arena were calculated. The rate of recording: 3 frames/s, center area: 30%.

Supplemental references

Omoto, Y., Lathe, R., Warner, M., and Gustafsson, J.-Å. (2005). Early onset of puberty and early ovarian failure in CYP7B1 knockout mice. Proc. Natl. Acad. Sci. U. S. A. *102*, 2814-2819.

Oyola, M.G., Zuloaga, D.G., Carbone, D., Malysz, A.M., Acevedo-Rodriguez, A., Handa, R.J., and Mani, S.K. (2015). CYP7B1 Enzyme Deletion Impairs Reproductive Behaviors in Male Mice. Endocrinology *156*, 2150-2161.